ACS APPLIED ENERGY MATERIALS
Cite This: ACS Appl. Energy Mater. XXXX, XXX, XXX−XXX
Article
www.acsaem.org

Multilayered WO_3 Nanoplatelets for Efficient Photoelectrochemical Water Splitting: The Role of the Annealing Ramp

Arlete Apolinário,[†,‡] Tânia Lopes,[†] Claúdia Costa,[†] João P. Araújo,[‡] and Adélio M. Mendes*[,†]

[†]LEPABE, Departamento de Engenharia Química, Faculdade de Engenharia da Universidade do Porto, Rua Dr. Roberto Frias, 4200-465 Porto, Portugal

[‡]IFIMUP and IN-Instituto de Nanociência e Nanotecnologia, Departamento de Física e Astronomia, Faculdade de Ciências da Universidade do Porto, Rua do Campo Alegre, 678, 4169-007 Porto, Portugal

Supporting Information

ABSTRACT: Multilayered WO_3 nanosquare platelet films were successfully grown on transparent TCO substrates by spray-coating WO_3 nanoparticles aqueous suspension prepared by the sol−gel method. This work assesses the influence of two annealing schemes in the photoresponse of WO_3 photoelectrodes with different film thicknesses. The photoelectrochemical characterization reveals that the slow-heating ramp produces a photoelectrode with an improved photocurrent density of 1.6 mA cm^{-2} at 1.23 V vs RHE. Comparing photoelectrodes with the same film thickness, the slow-heating ramp yields higher photocurrent densities, 80% more than the conventional fast-heating ramp. The effect of the annealing ramp on the morphology and crystalline-phase structure of WO_3 photoelectrodes is correlated with the photocurrent density. The slow-heating ramp annealing unveils film morphology with both higher porosity degree and higher nanosquare platelets dimensions. X-ray diffraction (XRD) structural analyses disclose that the films grow in monoclinic crystalline phase with a textural preferential direction [002], often related to improved photocurrent performances. The crystallite sizes and lattice microstrain are estimated using a simple X-ray diffraction broadening method, the Williamson-Hall analysis. A quantified correlation between the WO_3 lattice defects, intergrain strains, and performance is done. The proposed deposition method paves the way for producing efficient and scalable photoelectrodes of WO_3 for photoelectrochemical water splitting by using low-cost and simple manufacturing processes.

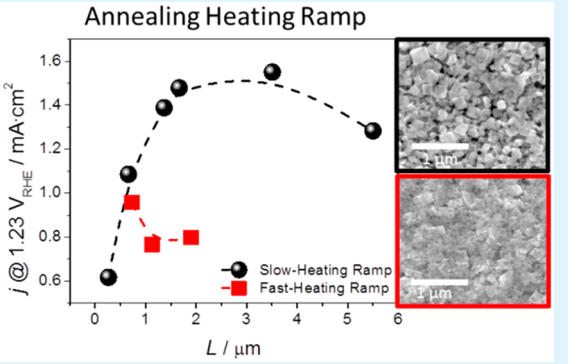

KEYWORDS: *photoelectrochemical cells, tungsten trioxide, photoelectrodes, nanoplatelets, annealing ramp, X-ray peak broadening*

INTRODUCTION

One of the greatest challenges of the 21st century is to reduce the greenhouse gas emissions while keeping the standard of living.[1] Sunlight is by far the most abundant renewable source of energy, exceeding the potential of all other energy sources and capable of supplying the present and projected world's energy demands.[2] Nonetheless, solar technologies have played a limited role in the current energy context mainly due to the lack of availability of cost-effective and efficient technologies for storing energy;[3] storage solutions are particularly important to mitigate the intermittency of solar energy and to ensure the stability of the electrical grid.[4]

Hydrogen production via photoelectrochemical (PEC) water splitting is a promising approach since it combines the solar harvesting, conversion, and storage functionalities all in one, which is favorable in terms of packaging and overall system costs.[5,6] However, to be a competitive alternative for producing sustainable hydrogen, earth-abundant photoelectrode materials have to be considered that simultaneously are highly energy efficient and chemically stable under sunlight and low-cost.[7,8] Accordingly, the photoelectrode must comply with several requirements: proper band gap energy (~2 V), settled to cover the water dissociation energy (1.48 eV), the thermodynamic losses as well as the overpotentials; broad absorption over the visible light range; fast transport of the photogenerated charges (high carriers mobility) and long electron−hole pair diffusion length; adequate band edge positions either to assist oxidation and reduction of water; chemical and electrochemical stability in water and under illumination and low cost.[8,9]

The first semiconductor recognized to split water was TiO_2 under UV light irradiation, reported by Fujishima and Honda in 1972.[10] Thenceforward, several semiconducting materials have been extensively investigated, eager to find the ideal photoelectrode material that could directly split water into hydrogen and oxygen by light-induced electrochemical processes.[11] In fact, only a few semiconductor materials hold a suitable bandgap and appropriate band edges for operating at

Received: September 11, 2018
Accepted: January 10, 2019
Published: January 10, 2019

DOI: 10.1021/acsaem.8b01530
ACS Appl. Energy Mater. XXXX, XXX, XXX−XXX

zero bias, e.g., Ta_3N_5[12] and CdS. Nevertheless, these materials do not fulfill the stability requirement.[13] Presently, much attention is given to the improvement of metal oxide semiconductors that are generally stable, able to photooxidize water (O_2 evolution) with a fairly easy synthesis process, and scalable.[8] Particularly, n-type metal oxide semiconductors are very promising since it facilitates hydrogen gas collection at the metal-counter electrode, which is important for the large-scale application. Accordingly, research on semiconductor photoanodes for solar hydrogen production via PEC water splitting is nowadays mainly focused on three different materials:[14] tungsten trioxide (WO_3),[14,15] bismuth vanadate ($BiVO_4$),[16] and hematite (α-Fe_2O_3).[9,13] In recent years, α-Fe_2O_3 and WO_3 have gained relevance due to their excellent chemical stability in aqueous media, low cost, raw material availability, and fairly easy synthesis.[8,9,17] Hematite, with a suitable band gap of 2.1−2.2 eV allows one to collect up to 40% of the solar spectrum energy.[9,13] However, it displays poor electron mobility (0.01−0.1 $cm^2\ V^{-1}\ s^{-1}$), resulting in short charge carrier diffusion lengths (2−4 nm).[8] Tungsten trioxide, has been widely investigated for different applications such as photocatalysis, photochromism, and sensing.[18] Although, WO_3 displays a broader band gap, 2.7−2.8 eV, which may limit the absorption of the solar spectrum, it shows a higher electron mobility (6 $cm^2\ V^{-1}\ s^{-1}$) and longer charge carrier diffusion lengths (∼150 nm) making this photoanode material a more promising candidate.[8] Nanostructuring has emerged as one of the best tools to enhance these advantages allowing at the same time narrowing the band gap.[17−21] By controlling the nanostructure architecture, the interface and thus the contact between the electrode and electrolyte can be improved. In fact, the charge transport efficiency can be enhanced (electron pathways and hole diffusion to the surface), and the exposed photoactive surface area can be highly increased, improving the absorption of visible light.[9,19,22] Moreover, the WO_3 photoelectrode crystallinity, grain boundaries, defects, and impurities are key-features for an efficient charge separation, transport, and collection that leads to higher photocurrents and photovoltages.[17,19,23] Nonetheless, to the best of the authors' knowledge, it has not yet been reported that there is a quantified correlation between the WO_3 lattice defects, intergrain strains, and the photo-to-current performance.

Different synthesis methods for preparing nanostructured WO_3 photoelectrodes have been widely explored, specifically by physical, electrochemical, and chemical routes: (i) sputtering (reactive rf magnetron) and thermal deposition;[24−26] (ii) electrochemical anodization and electrodeposition;[27−29] (iii) sol−gel, hydrothermal, solvothermal, chemical vapor deposition, and spray-pyrolysis.[14,30−40]

The WO_3 photoelectrodes obtained by sputtering deposition (physical route) usually leads to high-quality photoanodes in terms of good crystallinity, less intergrain boundaries, and lattice defects.[24,25] In fact, Marsen et al. obtained a column-like morphology leading to one of the best photocurrents in the literature, j = 2.7 mA cm^{-2} at 1.6 V vs SCE (under 100 mW cm^{-2} illumination).[25] Still, this technique is expensive (high vacuum is required), and it is not easily scalable.

Electrochemical anodization of metallic W foils originates with WO_3 nanoporous or wormlike structures exhibiting photocurrent densities of ∼2 mA cm^{-2} at 1.5 V vs SCE (under 100 mW cm^{-2} illumination).[29] The electrochemical anodization is a low cost and scalable technique but presents some disadvantages: WO_3 grows on a nontransparent substrate (metallic W foil), and the nanostructure growth (growth-rate) and shape are directly affected by the foil roughness[41] (pretreatments procedures are required prior to anodization process) and by purity level of the foil.[42] WO_3 continuous films can be obtained by cathodic electrodeposition directly onto transparent conductive oxide (TCO) glass substrates. Though low cost and scalable, this method originated so far at much lower photocurrent densities, ∼0.35 mA cm^{-2} at 1.2 V vs Ag/AgCl.[43]

Promising results have been obtained via chemical route (iii). The solvothermal (including hydrothermal) is a simple fabrication method capable of producing different types of nanostructures, grown directly upon the TCO substrates. Through the solvothermal methods, flake-wall, nanomultilayers films and nanowire nanostructures can be found in the literature, producing photocurrent densities of 1.8 mA cm^{-2} at 1.4 V vs RHE, 1.6 mA cm^{-2} at 1.4 V vs RHE, and 1.4 mA cm^{-2} at 1.45 V vs Ag/AgCl, respectively (all under 100 mW cm^{-2}).[30−32] Through the hydrothermal technique it can be obtained uniform nanosized nanocrystals,[33] platelike, wedge-like, and sheetlike,[34] or nanorods[44] with reported photocurrent densities of 2.7 mA cm^{-2} at 1.4 V vs RHE, 0.5 mA cm^{-2} at 1.45 V vs Ag/AgCl, and of 2.26 mA cm^{-2} at 1.23 V vs RHE, respectively (under 100 mW cm^{-2}).

The most common method to prepare WO_3 films via the chemical route is by the sol−gel process.[14,35,36] Here, thicker nanocrystalline WO_3 films consisting of a network of WO_3 nanoparticles are obtained by several consecutive depositions (by the doctor-blade method) of a colloidal precursor solution ((poly)tungstic acid) onto the FTO substrate and subsequently followed by a thermal annealing. Thicker films with a high degree of porosity are formed by sequential applications of the precursor and annealing in a layer-by-layer approach, leading to photocurrent densities of 2.9 mA cm^{-2} at 1.23 vs RHE under 100 mW cm^{-2}.[14,35]

Recently Niederberger et al. obtained the best photocurrent density ever reported for bare WO_3 photoanodes using commercial powders applied by the doctor-blade method, j = 3.5 mA cm^{-2} at 1.23 vs RHE under 100 mW cm^{-2}. Features like the optimized nanostructuring of the photoanodes are indicated as a possible reason for this high performance.[45]

$I-V$ measurments using different electrolytes lead to different photocurrents, which points out for an oxidation of the electrolyte rather than the oxidation of water. Choi et al.[14,45−47] and Mi et al. findings showed that the electrolytes with ions such as CH_3CO^{2-}, Cl^-, PO_4^{3-}, SO_4^{2-}, are preferably photooxized (depending on pH) up to the complete suppression of the O_2 evolution.[46,47] Recently, electrolytes containing $CH_3SO_3^-$, which hold the photocurrent benchmark, led to contradictory conclusions.[14,45] In fact, O_2 evolution measurements using 1 M CH_3SO_3H electrolyte were performed to evaluate the Faradaic efficiency that the WO_3 photoanode splits water into O_2; Augustynski et al.[14] obtained a Faradaic efficiency near 100% and Niederberger et al.[45] close to 0%.

Solvothermal, hydrothermal, and sol−gel are, in principle easy to scale techniques, displaying very promising photocurrent densities. Though, the synthesis procedure demands quite a few deposition stages (layer-by-layer approach), with several annealing steps, that ultimately lead to the increase of the WO_3 photoelectrode cost. Therefore, WO_3 photoelectrode price-to-performance ratio should be improved for the future commercialization of WO_3-based PEC devices. In fact, a

DOI: 10.1021/acsaem.8b01530
ACS Appl. Energy Mater. XXXX, XXX, XXX−XXX

chosen material for a PEC device must comply with three key requirements: efficiency, stability, and scalability.[48] Accordingly, research and development on nanostructured WO_3 should improve its physicochemical characteristics to obtain high-purity crystalline nanostructures (for efficient and stable photoanodes) bearing into consideration factors of great relevance: reduced costs; facile and scalable syntheses methods; and broad and fancy flexibility for design applications.[48]

Regardless the WO_3 photoelectrodes preparation method a thermal annealing is required to convert the WO_3 from disordered (amorphous) to ordered lattice (well-crystallized). Typically, for water splitting applications, such a transformation process significantly increases the photocurrent conversion efficiency, as the band gap energy decreases and the number of defective sites and surface states are reduced.[19,21,23] Furthermore, the monoclinic I (g-WO_3) is the most desirable crystallographic phase since it is the most stable at room temperature (in bulk WO_3).[17] Several efforts have been undertaken to find the best annealing conditions in WO_3 preparation. Thus, parameters such as temperature, time, and atmosphere have been explored to obtain the best photocurrent output. Generally, the thermal annealing temperature has a significant influence on WO_3 films morphologies and particle and crystallite sizes.[49−51] Modifications on WO_3 films morphologies occurred by varying the annealing temperatures: NPs layers changed from long needle-, small plate- to large-like (400−600 °C),[50] while anodized WO_3 films changed to rod-, sheet-, and fibril-like structures (250−500 °C).[49] In addition, particles (30−500 nm) and crystallite (37−129 nm) sizes increased with annealing temperature (500−800 °C),[51] ultimately influencing the photocurrent. Optimal annealing temperatures to obtain the best performances depend on the WO_3 preparation method since the thickness, structure, and morphology influences the effectiveness of the crystalline conversion.[17,25,44,49−53]

Additionally, a gradual photocurrent increase with the annealing time (1−3 h), in air atmosphere, was observed by Parker et al. This was ascribed to the oxygen deficiency increase in the lattice induced by the water content removal from the material during the annealing.[54] Varying the annealing atmosphere from air to H_2 (low degree of oxygen) or O_2 (high degree of oxygen) resulted in a photocurrent decrease for both scenarios. While the H_2 atmosphere provides a higher level of oxygen deficiency on the WO_3 photoelectrodes, increasing the defective sites and consequently e-h recombination, the O_2 atmosphere provides a low level of oxygen deficiency.[54] Furthermore, so far no relation with the annealing heating ramp has been performed.

In this work, an extremely simple, inexpensive, and easily scalable deposition method is presented. Multilayered WO_3 nanosquare platelets were successfully grew onto transparent TCO substrates by spray-coating a WO_3 nanoparticle suspension obtained by the traditional sol−gel method. Special interest was given to the optimization of the annealing and sample thickness parameters. In particular, two sets of samples with different annealing heating-ramps, a conventional fast-heating ramp (FHR) and a slow-heating ramp (SHR), combined with the WO_3 film thickness variation were studied to produce an optimized WO_3-based photoelectrode for water splitting.

EXPERIMENTAL SECTION

WO_3 Photoelectrodes Synthesis. Tungsten oxide nanoparticles (NPs) were prepared by the sol−gel method. Metallic tungsten powder was added to hydrogen peroxide (30%) and allowed to react for approximately 3 min until a transparent colorless solution was formed; the solution was neither mixed nor heated during the reaction process. Afterward, it was heated up to 90 °C in a stirred vessel becoming first a yellow solution (after 2 h) and then pale-yellow precipitate (after 7 h). In the end, the yellow precipitate of tungsten trioxide nanoparticles was grounded with a mortar and then dispersed in water/ethanol (99%) (3:1 molar), originating a stable colloidal suspension with a concentration of 1.7 g dm^{-3}.[55]

The WO_3 photoelectrodes were prepared from the WO_3 nanoparticles (NPs), which were applied onto heated TCO-glass substrates (130 °C) by spray-coating (samples area of 2.5 cm^2). The NPs suspension was sprayed for 15 s followed by a 3 min pause; several cycles were performed until the desired volume of suspension was deposited. Different samples were prepared by varying the deposition volume. Depositions occurred at a fixed distance of 20 cm with a gun pressure (Wuto-7902-BL) of 4 bar (synthetic air). Afterward, the as-prepared WO_3 samples were annealed at 550 °C during 1 h in air; different heating ramps were applied. The annealed samples were then allowed to cool naturally to RT by switching off the oven. Parameters, WO_3 thicknesses and heating-ramp temperature, were optimized for producing the highest photocurrent at 1.23 V_{RHE}.

Photoelectrochemical, Morphology and Structural Characterization. The photoelectrochemical characterization was performed using a "cappuccino" cell.[11], made of polyetheretherketone (Erta PEEK), equipped with 20 mm diameter uncoated fused silica window (Robson Scientific, England) pressed against an O-ring by a metallic window part. The WO_3 photoelectrodes were immersed (approximately 2.5 cm^2) in an aqueous electrolyte made of 3.0 M methanesulfonic acid (MSA), pH 0.14, at 25 °C.[14,35] The measurements were performed using a standard three-electrode configuration: Ag/AgCl/saturated KCl electrode (Metrohm, Switzerland) as the reference electrode; a platinum wire as the counter-electrode (99.9% pure platinum wire (Alfa Aesar, Germany), and the WO_3 photoelectrode as the working electrode. The photocurrent−voltage (j−V) characteristic curves were obtained by applying an external potential bias to the cell and measuring the generated photocurrent using a ZENNIUM workstation (Zahner Elektrik, Germany) controlled by Thales software (Thales Z 2.6). The measurements were performed in the dark and under 1-sun simulated sunlight (illuminated area of 0.58 cm^2), at a scan rate of 10 mV s^{-1} between 0.4 and 1.8 V_{RHE}. A class B solar simulator equipped with a 150 W Xe lamp (Oriel, Newport) and an AM 1.5 G filter (Newport) was used, and the light beam was calibrated with a c-Si photodiode (Newport) to 100 mW cm^{-2} (Figure S5). The WO_3 photoelectrodes thickness (L) was obtained using a profiler (Dektak XT, Bruker). The morphology was assessed using scanning electron microscopy (FEI Quanta 400FEG Field Emission). To determine the NPs dimensions from the SEM images, a freeware processing image software *ImageJ* was used.[56] The structural characterization was made using X-ray diffraction (XRD, *Rigaku* SmartLab) with Cu K_α radiation (1.5406 Å); both Bragg-Brentano (BB) focusing and parallel-beam (PB) methods were used.

RESULTS AND DISCUSSION

Photoelectrochemical Performance: j−V Characteristic Curves. Several WO_3 photoelectrodes were prepared with different thicknesses and with two distinctive heating ramps for the annealing procedure, a FHR of 500 °C h^{-1} and a SHR of 60 °C h^{-1} (Table 1). The j−V characteristic curves under dark and illumination conditions were obtained for these photoelectrodes (Figure 1). Generally, samples prepared with the SHR display better performance. Furthermore, the current density (j) for the SHR samples increases as L increases, while for the FHR samples j decreases. On the other hand, for the

DOI: 10.1021/acsaem.8b01530
ACS Appl. Energy Mater. XXXX, XXX, XXX−XXX

Table 1. Sets of Prepared Samples: Different Deposited Volume

deposited volume (mL)	L (μm)
Slow-Heating Ramp	
20	0.26
40	0.66
60	1.4
80	1.7
100	3.5
120	5.5
Fast-Heating Ramp	
40	0.73
60	1.1
80	1.9

SHR samples, the optimum performance was observed for $L \approx 3.5$ μm with a current density under an illumination of 1.6 mA cm^{-2} at 1.23 V_{RHE}. However, further thickness increase (L = 5.5 μm) led to a j decrease (1.3 mA cm $^{-2}$).

Furthermore, comparing photoelectrodes with approximately the same thickness, (e.g., L = 1.1 and 1.3 μm, 1.9 and 1.7 μm for fast and slow heating ramp schemes, respectively) the ones with a SHR leads to a photocurrent improvement of more than 80% compared to the ones with conventional FHR thermal annealing. The onset potential under illumination for the prepared samples is between 0.5 and 0.6 V_{RHE} (typical range found in the literature[14]); and for the sample with the best performance a value of 0.55 V_{RHE} was obtained. For the as-prepared WO_3, the current density under illumination is only slightly higher than that one presented under dark conditions, indicating that the material is not photoactive (Figure 1a).

Oxygen evolution measurements were performed to confirm that the MSA electrolyte (containing $CH_3SO_3^-$) is not photooxidized and thus not overestimating j. A faradaic efficiency of 80% was obtained, corroborating the studies of Augustinsky et al. that obtained a faradaic efficiency close to 100%.[14]

WO_3 Photoelectrode Morphology Analysis. SEM images reveal that the WO_3 NPs suspension sprayed on the TCO substrates grows as continuous porous films composed by multilayers of nanoplatelets (Figure 2). For the as-prepared sample, a film of NPs with a shallow parallelepiped geometry with a mean edge square (s) ~200 nm was obtained (Figure 2a,d). Moreover, when a FHR is considered, the samples display merged NPs, which originate from a blurred surface image, and films exhibit lower porosity as illustrated in Figure 2b,e) It is worth mentioning that the morphology of the three samples are equivalent, only the thickness is different, see Figure S1 in the Supporting Information. On the other hand, the samples annealed with the slow heating ramp exhibit smaller nanoplatelets with rounded square geometry, where the mean edge is ~150 nm (Figure 2c) and the mean height (t) is ~50 nm (Figure 2f), and the films show high porosity

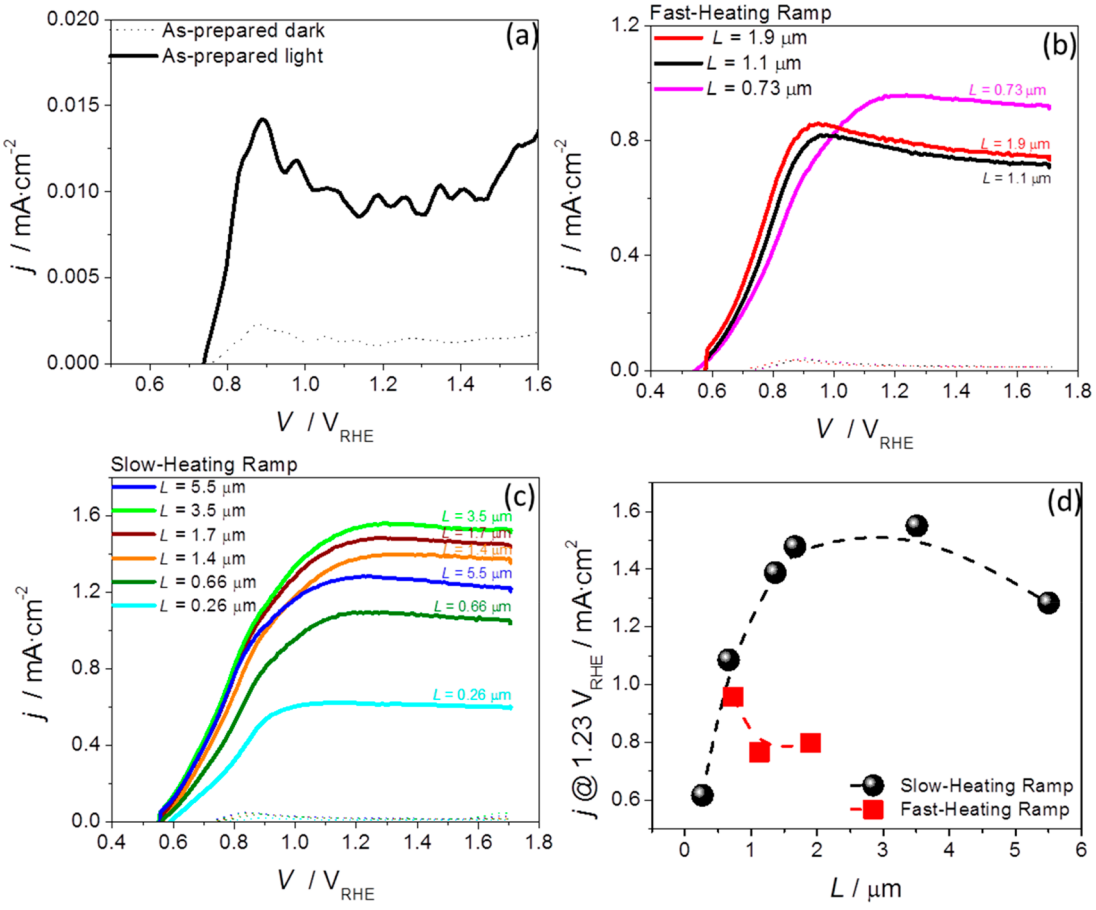

Figure 1. j–V characteristic curves for WO_3 photoelectrodes: (a) as-prepared; (b) annealed with a fast-heating ramp, 500 °C h^{-1}; and (c) annealed with a slow heating-ramp, 60 °C h^{-1}; in the dark (dashed lines) and under 1 SUN 100 mW cm^{-2} light conditions (full lines). (d) WO_3 photoelectrodes thickness (L) as a function of j at 1.23 V_{RHE} for the fast and slow heating ramp.

DOI: 10.1021/acsaem.8b01530
ACS Appl. Energy Mater. XXXX, XXX, XXX−XXX